Erschienen in: Biochimica et Biophysica Acta : Proteins and Proteomics ;
1814 (2011), 7. - S. 873-881
https://doi.org/10.1016/j.bbapap.2011.03.016

NMR relaxation unravels interdomain crosstalk of the two domain prolyl isomerase and chaperone SlyD

Michael Kovermann [a,b], Robert Zierold [a,1], Caroline Haupt [a,b], Christian Löw [c], Jochen Balbach [a,b,*]

[a] *Institut für Physik, Biophysik, Martin-Luther-Universität Halle-Wittenberg, D-06099 Halle (Saale), Germany*
[b] *Mitteldeutsches Zentrum für Struktur und Dynamik der Proteine (MZP), Martin-Luther-Universität Halle-Wittenberg, D-06099 Halle (Saale), Germany*
[c] *Department of Medical Biochemistry and Biophysics, Karolinska-Institutet, SE-17177 Stockholm, Sweden*

Keywords:
Protein folding
Prolyl isomerase
Molecular chaperone
FKBP
NMR dynamics
Diffusion

A B S T R A C T

The dynamics of the two domain prolyl peptidyl *cis*/*trans* isomerase and chaperone SlyD was studied on a ps to ns time scale to correlate dynamic changes with the catalytic function. ^{15}N transversal and longitudinal relaxation rates as well as heteronuclear Overhauser effects were determined at different temperatures for *Escherichia coli* SlyD (*Ec*SlyD) and for *Thermus thermophilus* SlyD (*Tt*SlyD). With the well established extended Lipari Szabo approach, the order parameter, S^2, the internal correlation time, τ_e, the exchange rate, R_{ex}, of the backbone amide protons, and the overall molecular tumbling time, τ_m, were determined. The study was extended to a relaxation analysis of the peptide bound state for both SlyD species. We found highly different relaxation and dynamic behavior of the two domains for free SlyD. Surprisingly, in the presence of a substrate for the chaperone domain, the ps to ns dynamics in the remote center of the prolyl peptidyl *cis*/*trans* isomerization domain increases. We observed this crosstalk between the two domains for both *Ec*SlyD and *Tt*SlyD.

1. Introduction

To understand the molecular mechanisms of protein function, stability, and activity, the three dimensional structure of a protein and the knowledge of different modes of motions are of high benefit [1 4]. NMR spectroscopy provides different experiments to probe both protein structure and dynamics. Exceptional are the different dynamic time scales covered by NMR to observe any kind of molecular motion [5], which span more than 12 orders of magnitude, from picoseconds up to hours and days [4,6 8]. Concerning the range of very fast tumbling, the majority of work was performed on single domain proteins and model systems suitable for NMR in terms of molecular size [9 12]. Recently, a direct link between dynamics and biological function for larger proteins was theoretically [3,13 15] and experi mentally [16] tackled. Also, recently, Byeon et al. [17] and Marston et al. [18] reported on allosteric and interdomain communication revealed by NMR.

In this paper, we present a ^{15}N NMR relaxation study of the 20 kDa 2 domain protein SlyD (Fig. 1), which is a peptidyl prolyl *cis*/*trans* isomerase [19]. SlyD (acronym for "sensitive to lysis D"), discovered in *Escherichia coli* as a host factor for the bacteriophage ΦX174 lysis cycle [20], has been identified as a cytoplasmic peptidyl prolyl *cis*/*trans* isomerase (PPIase) [21] of the FK506 binding protein family (FKBP domain) and as a particularly efficient chaperone (IF domain) [22,23]. Recent structural work showed that the two domains of SlyD experience a different level of protection against exchange with the solvent (for *Ec*SlyD, C.H. and J.B. to be published elsewhere; for *Thermus thermophilus* SlyD, C. Löw et al. [24]), no distinct domain orientation relative to each other [22,25], a clear difference in folding and unfolding rates [26] but an assistance during catalysis[27]. Also, recently, we have shown a tight interaction between *Tt*SlyD and the Tat (twin arginine translocation) signal peptide [24]. During the Tat dependent translocation of folded substrates from the cytosol to the periplasm of *E. coli*, SlyD interacts with the unstructured Tat signal peptide of the substrate, protecting it from proteolytic degradation in the cytosol [28].

For the present study, we used truncated *Ec*SlyD (1 165) (*Ec*SlyD*) because the C terminus is not structured and does not modify the PPIase and molecular chaperone function [22,25]. This corresponds to wildtype SlyD (1 148) from *T. thermophilus*, which lacks these C terminal residues. ^{15}N NMR relaxation data for *Tt*SlyD and *Ec*SlyD* were recorded in free as well as in a Tat peptide bound state. We

Abbreviations: SlyD, product of the *slyD* (sensitive-to-lysis) gene; *Ec*SlyD*, 1–165 fragment of *Escherichia coli* SlyD; *h*FKBP12, human FKBP12; IF, insert in flap; *Ec*SlyD*ΔIF, variant of *Ec*SlyD* in which the IF domain is replaced by the flap of human FKBP12; *Tt*SlyD, full-length protein of *Thermus thermophilus* SlyD; *Tt*SlyDΔIF, variant of *Tt*SlyD in which the IF domain is replaced by the flap of human FKBP12; Tat, twin-arginine-translocation

* Corresponding author at: Institut für Physik, Fachgruppe Biophysik, Martin-Luther-Universität Halle-Wittenberg, Betty-Heimann-Str. 7, D-06120 Halle (Saale), Germany. Tel.: +49 345 55 28550; fax: +49 345 55 27161.
E-mail address: jochen.balbach@physik.uni-halle.de (J. Balbach).
[1] Current address: Institut für Angewandte Physik, Universität Hamburg, D-20355 Hamburg, Germany.

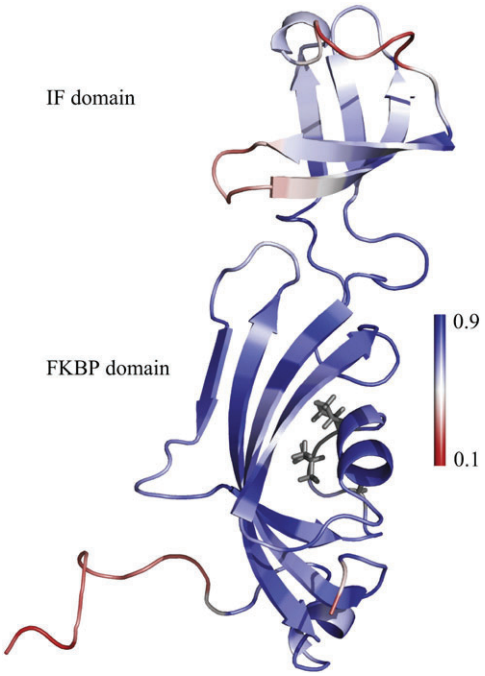

Fig. 1. Domain architecture of *Ec*SlyD* according to the NMR derived structure (lowest energy structure of pdb entry 2K8I). The color coding corresponds to the heteronuclear NOE values at $T = 298$ K and $B_0 = 14.1$ T ranging from red (hNOE = 0.1) via white (hNOE = 0.55) to dark blue (hNOE = 0.9). G39, L41, and I42 in the FKBP domain, which are dynamically most affected upon peptide binding to the IF domain, are shown in a gray stick representation. Note that, according to the NMR structure calculation, there is no defined orientation of the FKBP domain (K2–V62, Q128–G150) and the IF domain (L75–D120).

interpreted the relaxation parameters of the backbone amide protons with the well established model free approach [29 31] in the light of the two spatially separated functions of SlyD. In addition, we recorded diffusion profiles [32] for *Ec*SlyD*, *Ec*SlyD*ΔIF, *Tt*SlyD, *Tt*SlyDΔIF, and human FKBP12 to characterize shape and tumbling of these proteins. The mechanism of communication between the two domains during substrate interaction was further studied by a titration experiment using the Tat signal peptide, detected via fluorescence and NMR spectroscopy. Beside binding events at distinct places in the protein, we observed changes in the dynamic behavior of SlyD. Interestingly, in the presence of the Tat peptide, the ns to ps dynamics at the center of the prolyl peptidyl *cis*/*trans* isomerization site increased, although Tat binding occurs at the other, remote IF domain.

2. Materials and methods

2.1. Proteins and peptides

A truncated variant of *Ec*SlyD (1 165, *Ec*SlyD*) and the full length wild type of *Tt*SlyD (1 148), both containing an additional His tag for purification, were expressed and purified as described before [23,24]. *Ec*SlyD*ΔIF as well as *Tt*SlyDΔIF were constructed by replacing the IF domain with the shorter flap sequence of human FKBP12 [33]. Human FKBP12 (*h*FKBP12) was cloned in a pET24a plasmid, transformed in *E. coli* BL21 (DE3) and expressed in M9 minimal medium containing 1 g/l ^{15}N NH_4Cl. His tagged *h*FKBP12 was purified by immobilized nickel ion chromatography (Ni sepharose; GE Healthcare) followed by size exclusion chromatography (Superdex 75; GE Healthcare). The protein concentration was 1.4 mM for the NMR relaxation study of *Ec*SlyD* and *Tt*SlyD (free form) as well as the diffusion study of *Ec*SlyD*, *Tt*SlyD, *Ec*SlyD*ΔIF, and *Tt*SlyDΔIF. Transient aggregation or dimerization at this concentration could be excluded by analytical ultracentrifugation. For the NMR relaxation studies of the Tat peptide/SlyD complexes, concentrations of 0.36 mM (*Ec*SlyD*) and 0.48 mM (*Tt*SlyD) were used. The protein concentration was 1 mM for diffusion measurement of *h*FKBP12.

For the NMR titration and the NMR relaxation experiments of the SlyD/Tat peptide complexes, we used a 17 amino acid long peptide (NH_2 QRRDFLKYSVALGVASA OH), purchased from Activotec, Cam bridge, UK. A 27 amino acid long fragment (NH_2 QRRDFLKYSVALG VASALPLWSRAVFA OH) was used (with the intrinsic fluorophore W21) for the fluorescence titration experiments and for a control NMR titration experiment, purchased from the same company.

2.2. NMR relaxation measurements

All NMR experiments were carried out on a Bruker 600 Avance II spectrometer, if not explicitly stated differently. Spectra were measured in 50 mM sodium phosphate and 100 mM sodium chloride, pH 7.5, containing 10% (vol./vol.) D_2O. Backbone resonances of $^{13}C/^{15}N$ labeled *Ec*SlyD* and *Tt*SlyD samples were previously assigned by standard triple resonance experiments HNCA, HNCACB, HN(CO)CACB [22,24]. For relaxation measurements, ^1H ^{15}N HSQC based standard sequences [34,35] with 1024×128 complex data points and 16 scans were used. The recycle delay was set to 1 s for R_1 and for R_2 relaxation and 3 s for the hNOE experiment. Pulse strengths of 150 kHz (proton channel) and 50 kHz (nitrogen channel) were chosen. The following relaxation delays were exploited: R_1 relaxation, 20 ms, 40 ms (3), 70 ms, 100 ms, 130 ms, 350 ms, 500 ms, 770 ms, 900 ms, 1105 ms, 1500 ms, 1800 ms (2), 2500 ms; R_2 relaxation: 8.08 ms, 24.24 ms, 40.4 ms (3), 56.56 ms, 72.72 ms, 88.88 ms, 105.04 ms, 137.36 ms, 169.68 ms (2), 202 ms, 234.32 ms. The number in brackets specifies the number of repetitions used for error estimation. For the steady state ^1H ^{15}N hNOE experiment, 600 saturation 120° pulses (each 5 ms long) to the proton channel were used to saturate the transition between protons and nitrogens.

The spectral widths for *Ec*SlyD* were set to 13.02 ppm (proton channel) and to 23 ppm (nitrogen channel); transmitter frequencies were adjusted to the water resonance (proton channel) and to 119 ppm (nitrogen channel). The spectral widths for *Tt*SlyD were set to 14.02 ppm (proton channel) and to 26.7 ppm (nitrogen channel); transmitter frequencies were placed to the water resonance (proton channel) and to 118 ppm (nitrogen channel). The temperatures used for relaxation analysis of *Ec*SlyD* were 288 K, 293 K, 298 K, and 303 K; for *Tt*SlyD, 288 K, 298 K, 303 K, 313 K, and 333 K.

The NMR titrations of the Tat peptide (1 17) were performed at 298 K under equilibrium conditions to both species of SlyD. After each titration step, a ^1H ^{15}N HSQC spectrum of ^{15}N labeled SlyD was acquired. The relaxation study of the Tat bound *Ec*SlyD* and *Tt*SlyD was performed at 298 K. All NMR spectra were processed using NMRPipe [36] and analyzed using NMRView [37].

2.3. ^{15}N relaxation analysis

The longitudinal, R_1, and the transversal relaxation rates, R_2, were derived by fitting a single exponential decay to the NMR intensities,

$$I(t) = I(0)\exp\left(-R_{1,2}t\right), \tag{1}$$

using the data analysis software IGOR (Wavemetrics) with scripts written in house. The errors of the relaxation rates, $\Delta R_{1,2}$, result from the mean relative error (determined from standard deviation of triplicate experiments) weighted regression of Eq. (1) to the peak intensities. The hNOE values were calculated by the ratio between the saturated experiment and the non saturated reference for each assigned amide proton. The error for the hNOE experiment was analyzed by using the standard deviation of three back to back recorded spectra.

2.4. Model free analysis

Calculations of motional parameters for *Ec*SlyD* and for *Tt*SlyD at 298 K according to the Lipari Szabo approach were performed with the program ModelFree [38,39] (version 4.22). The measured relaxation rates of the ^{15}N spins depend on a linear combination of frequency dependent spectral density functions, $J(\omega)$, and on the chemical shift anisotropy, $\Delta\omega$, of the ^{15}N nuclei [40]. The chemical shift tensor is assumed to be axially symmetric. A conventional value of $\Delta\omega$ is −160 ppm [41], which has been used for the Lipari Szabo analysis.

Because of non isotropic symmetry of the 2 domain proteins *Ec*SlyD* and *Tt*SlyD, we used an axially symmetric model, which describes the structure of both species [22,24] well. Starting parameters (overall tumbling time, τ_m; ratio of diffusion axes, $D_{\parallel}/D_{\perp}$; polar angles theta, θ; and phi, ϕ) for the axial symmetric model calculation in ModelFree were determined by usage of the software package TENSOR2 [42] with input of the NMR or crystal structure of *Ec*SlyD* and *Tt*SlyD, respectively.

The extended Lipari Szabo approach uses five different spectral density functions, $J(\omega_i)$, differently depending on the dynamic order parameter, S^2, S_s^2, S_f^2; the internal correlation time, τ_e; the overall (protein) correlation time, τ_m; and on a chemical exchange rate, R_{ex}; see Table 1. We calculated for every assigned ^{1}H ^{15}N vector all five models and performed the model selection as described [39,43], with MatLab (MathWorks) scripts written in house.

2.5. NMR diffusion measurement

NMR diffusion spectra were recorded by pulsed field bipolar gradient stimulated echo experiments [32] at a proton resonance frequency of 600 MHz. For each diffusion profile, 21 different gradient strengths, G, were used for 6 ms along the z axis, followed by a 100 μs recovery delay. The diffusion of protein molecules was allowed to proceed for 140 ms to ensure a protein signal intensity decay of approximately 95% at the highest gradient strength. The calibration of absolute gradient strengths was performed by a standard protocol [44]. For error estimation, four different gradient strengths were repeated (relative gradient strengths of 1%, 10%, 40%, and 70%). The measured ^{1}H NMR spectra were integrated between 0.5 and 2.5 ppm (aliphatic region) as well as 6.5 and 8.5 ppm (amide proton region). Eq. (2) was adapted to these recorded data sets:

$$I(G) = I(0)\ exp\left(-G^2\gamma^2\delta^2 D(\Delta-\delta/3)\right), \tag{2}$$

Table 1
Models and associated spectral densities for the extended model-free analysis of ^{15}N relaxation data.

Model	Spectral density function	Optimized parameter(s)
1	$J(\omega) = \frac{2}{5}\left(\frac{S^2\tau_m}{1+(\omega\tau_m)^2}\right)$	S^2
2[a]	$J(\omega) = \left(\frac{S^2\tau_m}{1+(\omega\tau_m)^2} + \frac{(1\ \ S^2)\tau}{1+(\omega\tau)^2}\right)$	S^2, τ_e
3	$J(\omega) = \frac{2}{5}\left(\frac{S^2\tau_m}{1+(\omega\tau_m)^2}\right)$ $R_{2,obs} = R_{2,0} + R_{ex}$	S^2, R_{ex}
4	$J(\omega) = \frac{2}{5}\left(\frac{S^2\tau_m}{1+(\omega\tau_m)^2} + \frac{(1\ \ S^2)\tau}{1+(\omega\tau)^2}\right)$ $R_{2,obs} = R_{2,0} + R_{ex}$	S^2, τ_e, R_{ex}
5[a,b]	$J(\omega) = \frac{2}{5}\left(\frac{S^2\tau_m}{1+(\omega\tau_m)^2} + S_f^2\frac{(1\ \ S_s^2)\tau}{1+(\omega\tau)^2}\right)$	S_s^2, S_f^2, τ_e

[a] $\tau\ ^{1} = \tau_m\ ^{1} + \tau_e\ ^{1}$.
[b] $S^2 = S_s^2 S_f^2$.

where γ is the gyromagnetic ratio of protons, δ is the gradient length, Δ is the diffusion time, and D is the calculated diffusion coefficient [32,45].

Diffusion experiments were measured at a temperature of 298 K for *Ec*SlyD*, *Ec*SlyD*ΔIF, *Tt*SlyD, *Tt*SlyDΔIF, and *h*FKBP12. The mea sured value of the diffusion coefficient D was used for comparison to theoretical diffusion coefficients for globular proteins of the same size [46] via the calculation of the hydrodynamic radius [47], r_H, by Eq. (3):

$$D = \frac{k_B T}{6\pi\eta r_H}, \tag{3}$$

in which k_B is Boltzmann's constant and η is the viscosity of the solvent. The viscosity of the solvent was determined with a rheometer (RHEOPLUS/32 V3.31).

2.6. NMR titration

For the NMR titration experiments, the Tat peptide (1 17) was added stepwise up to a 2 fold excess of the peptide for the *Ec*SlyD* titration (0.73 mM:0.36 mM) and with a 1.3 ratio for the *Tt*SlyD titration (0.60 mM:0.48 mM). For every step during the titration, we followed the peak intensity and the chemical shift of every assigned protein cross peak in a series of ^{1}H ^{15}N F HSQC spectra [48]. The overall change of chemical shift values [49], $\Delta\delta^{all}$, was calculated with Eq. (4):

$$\Delta\delta^{all} = \sqrt{\frac{\left(\Delta^1H\right)^2 + {}^1\!/_{25}\left(\Delta^{15}N\right)^2}{2}}, \tag{4}$$

where Δ^1H is the change of the proton chemical shift and Δ^{15}N is the change of the nitrogen chemical shift.

Binding curves of the peptide to *Ec*SlyD* and to *Tt*SlyD were fitted to the recorded data sets with Eq. (5):

$$\Delta\delta^{all}(c) = -a\frac{(B + nc + K_D)^2 - B - nc - K_D + 4nc\sqrt{B}}{2B}$$
$$\text{with}: B = \frac{c_0 - c}{c_0^{pep}}, \tag{5}$$

where a is the maximum of $\Delta\delta^{all}$, K_D is the dissociation constant, n is the stoichiometry, c is the peptide concentration, c_0 is the start concentration of the protein, and c_0^{pep} is the concentration of the stock solution of the peptide.

The Tat (1 27) peptide was used at a concentration of 73.5 μM to study the interaction with 65 μM *Tt*SlyDΔIF by NMR at 298 K.

2.7. Fluorescence titration

All fluorescence spectra were recorded with a JASCO FP 6500 fluorescence spectrometer equilibrated at a temperature of 298 K. During the titration experiment of the Tat peptide (1 27), we increased stepwise the *Ec*SlyD* concentration and finished with an excess of the protein relative to the Tat peptide of 6.5 μM:1 μM. As a control experiment, we performed a titration of *Ec*SlyD*ΔIF and *Tt*SlyDΔIF (constructs without IF domain) to the Tat peptide (1 27). Here, the final ratios were 6.5 μM:1 μM and 4.9 μM:0.8 μM, respectively.

Eq. (6) was fit to the fluorescence quench, F, during the titration of *Ec*SlyD* to the Tat peptide (1 27),

$$F(c) = q\frac{p + nc + K_D - \sqrt{(p + nc + K_D)^2 - 4npc}}{2p}, \tag{6}$$

where q is the maximum of the fluorescence quench, p is the concentration of the Tat peptide (1 27) (approximately 1 μM during

the titration), c is the concentration of *Ec*SlyD*, n is the stoichiometry of binding, and K_D is the dissociation constant of the binding process.

3. Results

3.1. Relaxation data at different temperatures for EcSlyD*

For an extended investigation of the dynamics of *Ec*SlyD* in solution by NMR spectroscopy, R_1, R_2 rates, and steady state ^1H ^{15}N hNOE effects could be obtained for 136, 141, 137, and 141 backbone amides out of 159 non prolyl residues of the two domain protein at 288 K, 293 K, 298 K, and 303 K, respectively. Within this temperature range, *Ec*SlyD* is fully native [50]. Fig. 2a c shows all relaxation data plotted versus the protein sequence at 298 K (Supplementary Fig. SF1a c shows data at the 3 other temperatures 288 K, 293 K, and 303 K). Variations in all three relaxation parameters at all four temperatures reflect very nicely the domain structure of *Ec*SlyD*. The longitudinal relaxation rates, R_1, of the IF domain are increased up to a factor of 1.5 compared to the FKBP domain as well as the linker region and show maximal values of nearly 2.0 s^{-1} at the unstructured C terminus (Supplementary Fig. SF1a). Contrary, the transversal relaxation rates, R_2, of the backbone ^{15}N nuclei of the IF domain are lower compared to the FKBP domain (average of about 20 s^{-1}; Fig. 2b) and reach values of 10 s^{-1} that were also found at the C terminus. The temperature profile of the R_2 rates shows the same relative gradation (Supplementary Fig. SF1b). The hNOE values illustrate again that the two domains of *Ec*SlyD* experience different modes of motions on a ps to ns time scale. For several backbone amides in the IF domain, the hNOE value decreases down to a value of 0.2, whereas the FKBP domain comprises values above 0.6 (Figs. 1 and 2c). This is close to the upper theoretical limit of 0.83 at a magnetic field strength of 14.1 T and corresponds to a rotational correlation time of the molecule of approximately 14 ns.

Our relaxation data for *Ec*SlyD* confirm the structural separation in two domains of SlyD and prove recently published relaxation data of an N terminal fragment of *Ec*SlyD (1 146), recorded at B_0 of 18.8 T and 298 K [25].

The presented relaxation data for *Ec*SlyD* are sufficient to describe and understand dynamics on a ps to ns time scale of full length *Ec*SlyD because the C terminus is not structured and does not modify the PPIase and molecular chaperone function [22,23,25]. The R_1 and R_2 relaxation rates change upon temperature variation [51] (Supplementary Fig. SF1a and b) as expected for a molecule with a rotational correlation time of *Ec*SlyD*: decreasing R_2 rates and increasing R_1 rates by increasing the temperature (Table 2). The 10% trimmed weighted average value of the hNOE is not affected by temperature changes (Table 2 and Supplemen tary Fig. SF1c).

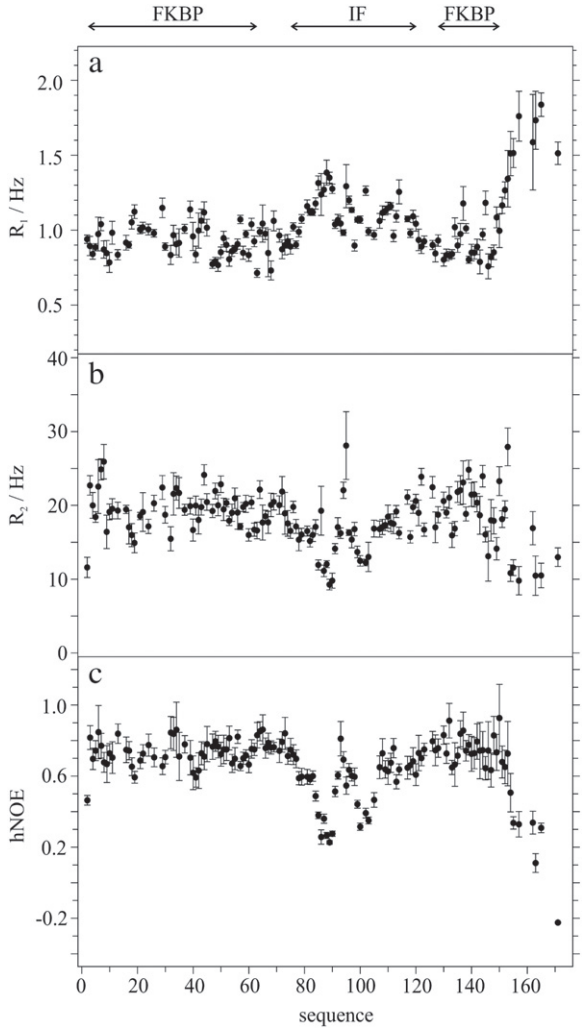

Fig. 2. NMR relaxation parameters of *Ec*SlyD* at $T = 298$ K and $B_0 = 14.1$ T. (a) Longitudinal ^{15}N relaxation rates, R_1; (b) transversal ^{15}N relaxation rates; and (c) ^1H-^{15}N heteronuclear NOE effects plotted against the amino acid sequence. The FKBP domain (K2–V62, Q128–G150) and the IF domain (L75–D120) are indicated at the top.

3.2. Relaxation data at different temperatures for TtSlyD

For *Tt*SlyD, we obtained relaxation data for 125, 124, 130, 124, and 121 backbone amides out of 138 non prolyl residues at 288 K, 298 K, 303 K, 313 K, and 333 K, respectively. Within this temperature range, *Tt*SlyD is fully native [24]. The IF and FKBP domain differ in the observed hNOE values and therefore in their local dynamics (Supplementary Fig. SF2c). However, the differences in the R_1 and R_2 rates between the two domains are much less pronounced (Supplementary Fig. SF2b and c) compared to *Ec*SlyD*. The overall temperature dependence of the 10% trimmed weighted average values of the relaxation rates and of the hNOE values is comparable to *Ec*SlyD* (Table 3).

3.3. Overall rotational correlation time and backbone dynamics of EcSlyD* and TtSlyD at different temperatures

The overall tumbling of protein molecules can be described by the rotational correlation time τ_m. A detailed analysis of τ_m and the backbone dynamics of *Ec*SlyD* and *Tt*SlyD at different temperatures was achieved by the Lipari Szabo approach using the measured R_1, R_2, and hNOE relaxation parameters. Model selection was achieved by an iterative protocol [39,43] with MatLab scripts written in house. The calculated values for τ_m decrease with increasing temperature (Tables 4 and 5). At 288 K, *Ec*SlyD* tumbles with a correlation time of motion, τ_m, of 15.1 ns and becomes (apparently) faster at a 15 K higher temperature ($\tau_m = 11.2$ ns). The viscosity correction for the buffer leads to a constant value for τ_m of about 13 ns for the entire temperature range (Table 4). For *Tt*SlyD, the overall tumbling was followed within a range of 45 K starting at 288 K. The rotational correlation time decreases (apparently) 4 fold from 19.3 ns down to 5.6 ns (Table 5). Herein, the viscosity correction of the buffer leads to

Table 2
Ten percent trimmed weighted average of the relaxation parameters for *Ec*SlyD* at four different temperatures.

	288 K	293 K	298 K	303 K
R_1/Hz	0.731	0.831	0.994	1.041
R_2/Hz	23.47	20.54	17.87	15.83
hNOE	0.640	0.667	0.686	0.680

R_1 indicateslongitudinal relaxation rate; R_2,transversal relaxation rate; hNOE, heteronuclear Overhauser effect.

Table 3
Ten percent trimmed weighted average of the relaxation parameters for *Tt*SlyD at five different temperatures.

	288 K	298 K	303 K	313 K	333 K
R_1/Hz	0.683	0.939	1.034	1.342	1.766
R_2/Hz	24.388	17.494	14.950	12.343	8.439
hNOE	0.675	0.696	0.705	0.709	0.716

R_1 indicates longitudinal relaxation rate; R_2,transversal relaxation rate; hNOE, heteronuclear Overhauser effect.

τ_m values, which decrease to higher temperatures contrary to *Ec*SlyD* and reach about 11 ns at elevated temperatures. Note that the ^{15}N relaxation data of both the 45 residue comprising IF domain and the FKBP domain could be analyzed by a single rotational correlation time. Separate model free runs of the individual domains resulted in very close τ_m values for both domains, indicating that they tumble as a single unit. This was not expected from the structure calculations, where no defined orientation between both domains was observed.

The parameters for the local motion of the polypeptide chain, S^2, τ_e, and R_{ex}, were derived from the extended Lipari Szabo analysis for *Ec*SlyD* at $T=288$ K, $T=293$ K, $T=298$ K (Fig. 3a c) and $T=303$ K. Over the entire temperature range, the FKBP domain of *Ec*SlyD* exhibits S^2 values above 0.8 and values close to 1 for most β strands as expected. The amide protons in the unstructured C terminus (starting at G150) experience large amplitude motions, with S^2 values below 0.4. The loop region of the IF domain shows a drop of S^2 from 0.95 down to values below 0.6 and only very few amides experience values close to 1, indicating increased amplitudes of motions of the IF domain. The values for the order parameter S^2 for *Tt*SlyD at 298 K give a less clear separation between the two domains compared to mesophilic SlyD but again only two residues of the IF domain reach values above 0.9 at this temperature (Supplementary Fig. SF3a).

The internal correlation time, τ_e, reflects fast internal motions of the protein additionally to the overall tumbling. During model selection according to Table 1, the majority of the amides in the IF domain of *Ec*SlyD* and *Tt*SlyD required models for all temperatures, which include these fast additional internal motions for a reliable interpretation of the ^{15}N relaxation data (model numbers 2, 4, and 5 in Table 1). Almost all of these τ_e values are at least one order of magnitude below τ_m (dashed line in Fig. 3b for *Ec*SlyD* and in Supplementary Fig. SF3b for *Tt*SlyD; both at 298 K). This is one of the prerequisites to generally apply the extended Lipari Szabo approach [30,31].

Several backbone amides reveal a chemical exchange contribution, R_{ex}, to the transversal relaxation rate for *Ec*SlyD* at 298 K, most of them below 3 Hz (Fig. 3c). These contributions monitor motions at a millisecond time scale. Interestingly, only few amides in the IF domain, which show strong τ_e contributions (around V76, A111, and D120), show additional motions at this slower time scale. For *Tt*SlyD, reduced R_{ex} contributions to the transversal relaxation (Supplementary Fig. SF3c for 298 K) with values below 1 Hz for most residues were found. These calculated exchange contributions reproduce the R_{ex} values directly obtained by usage of ^{15}N relaxation dispersion methods (data to be published elsewhere) very well. The overall course of the chemical exchange rate R_{ex} is not temperature dependent for both *Ec*SlyD* and *Tt*SlyD. Such a temperature independency of R_{ex} has been reported also, for example, for the B1 domain of *Streptococcal* protein G [9].

For *Ec*SlyD*, most favorable models for extended Lipari Szabo analysis are models 1 and 3 (within the whole temperature range; Supplementary Table ST1). For *Tt*SlyD, model 3 represents relaxation data best within the whole temperature range exceptionally at 288 K, where model 1 dominates (Supplementary Table ST2).

Table 4
Results for the extended Lipari–Szabo analysis for *Ec*SlyD*.

T/K	τ_m/ns	τ_m/η_{buffer}/ns	η_{buffer}/mPas
288	15.1 ± 0.1	12.8	1.18
293	13.7 ± 0.1	13.2	1.04
298	13.4 ± 0.1	13.4	1.00
303	11.2 ± 0.1	13.3	0.84

τ_m indicates rotational correlation time. The measured viscosity of the solvent, η_{buffer}, was used for correction according to the Stokes–Einstein relationship.

Table 5
Results for the extended Lipari–Szabo analysis for *Tt*SlyD.

T/K	τ_m/ns	τ_m/η_{buffer}/ns	η_{buffer}/mPas
288	19.3 ± 0.1	16.4	1.18
298	14.81 ± 0.04	14.8	1.00
303	11.0 ± 0.1	13.1	0.84
313	7.74 ± 0.02	11.1	0.70
333	5.63 ± 0.03	10.6	0.53

τ_m indicates rotational correlation time. The measured viscosity of the solvent, η_{buffer}, was used for correction according to the Stokes–Einstein relationship.

3.4. Diffusion coefficients

Diffusion measurements allow following the motion by translation, which is determined by the shape of the protein. Therefore, we

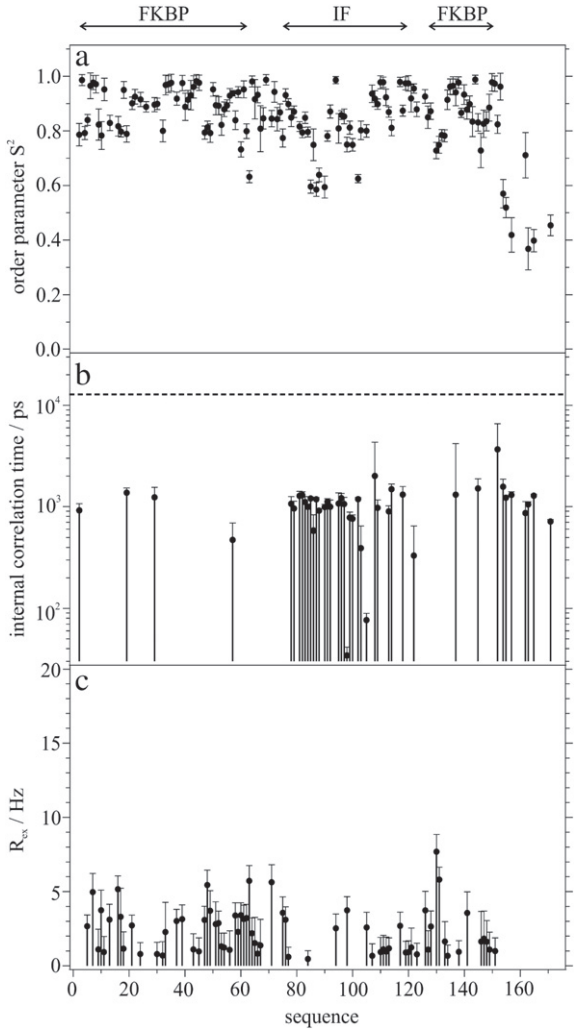

Fig. 3. Dynamic order parameter, S^2, (a); internal correlation time, τ_e, (b); and chemical exchange contribution, R_{ex}, to the transversal relaxation rate, R_2, (c), for *Ec*SlyD* at $T=298$ K and $B_0=14.1$ T. The FKBP domain and the IF domain are indicated at the top. In (b), the dashed line indicates the overall molecular tumbling time, τ_m.

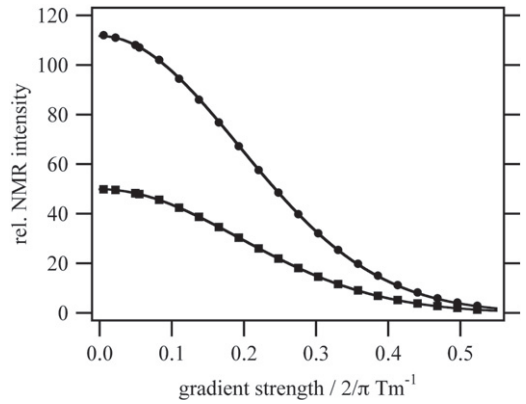

Fig. 4. Dependency of the NMR signal *I* on the gradient strength, *G*—running for the analysis of the diffusion coefficient, *D*—for *Ec*SlyD* (rectangles for measured data, straight line for fitting with Eq. (2)) and for *Tt*SlyD (circles for measured data and straight line for fitted data). For the NMR intensity, the resonances of the aliphatic signal region between 0.5 and 2.5 ppm in each ^{1}H spectrum were integrated.

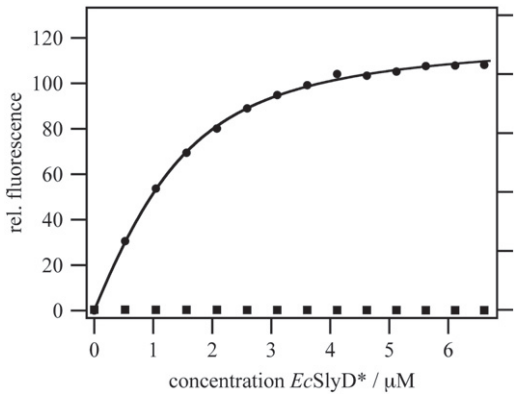

Fig. 5. Fluorescence titration of *Ec*SlyD* (circles) and of *Ec*SlyD*ΔIF (rectangles) to Tat peptide (1–27). The titration of *Ec*SlyD* to the peptide shows strong binding with a dissociation constant, K_D, of 400 ± 80 nM and a stoichiometry, *n*, of 0.8 ± 0.1. In contrast, the control titration of *Ec*SlyD*ΔIF to the peptide (1–27) shows clearly no binding.

measured the translational diffusion coefficient *D* for different SlyD variants (*Ec*SlyD*, *Ec*SlyD*ΔIF, *Tt*SlyD, *Tt*SlyDΔIF) and *h*FKBP12 [52,53], which structurally represents the FKBP domain of both *Ec*SlyD* and *Tt*SlyD, at 298 K (Fig. 4 and Table 6). The measured values for both two domain species are about the same, $D = (9.91 \pm 0.05)10^{-11}$ m^2 s^{-1} for *Ec*SlyD* and $D = (10.17 \pm 0.11)10^{-11}$ m^2 s^{-1} for *Tt*SlyD (these values are the average of the determined diffusion coefficients of aliphatic and amide protons). This consistency further verifies the use of truncated *Ec*SlyD* and wildtype *Tt*SlyD for this comparative study. To evaluate how the shape of the SlyD variants determines the translational diffusion, we calculated the expected theoretical diffusion coefficient from an assumed perfect spherical protein of the same number of residues at the same solvent viscosity (Eq. (3)) [46]. The presence of the IF domain reduces significantly the translational diffusion of both SlyD homologs which indicates an elongated shape of SlyD in solution as expected from the NMR and crystal structures.

3.5. Fluorescence titration of EcSlyD* and EcSlyD*ΔIF to Tat peptide (1 27)

During the Tat dependent translocation of folded substrates from the cytosol to the periplasm of *E. coli*, SlyD interacts with the Tat signal peptide of the substrate [28]. To study this SlyD/Tat peptide interaction *in vitro*, a titration experiment under equilibrium conditions was performed by following the change in intrinsic tryptophan fluorescence. Note that only the Tat peptide (1 27) contains one tryptophan residue whereas *Ec*SlyD* lacks this residue. We observed a tight binding of *Ec*SlyD* to the peptide (dissociation constant in the high nanomolar range) and a one to one binding stoichiometry (circles in Fig. 5). As a control experiment, we titrated *Ec*SlyD*ΔIF (well folded as confirmed by CD measurement and by diffusion (Table 6)) to the Tat peptide (1 27). For both experiments, no binding event was detectable (squares in Fig. 5). A fluorescence titration experiment for the respective thermophilic variants (*Tt*SlyD titrated to Tat peptide (1 27)) and control titration (*Tt*SlyDΔIF titrated to Tat peptide (1 27)) revealed analogous results as already reported [24].

Table 6
Diffusion analysis for different SlyD variants in comparison to *h*FKBP12 at 298 K.

Molecule	aa	D^{ali}/10 ^{11} m^2 s ^{1}	D^{aro}/10 ^{11} m^2 s ^{1}	D^{th}/10 ^{11} m^2 s ^{1}	D/D^{th}
*Ec*SlyD*	171	9.83 ± 0.04	9.96 ± 0.05	10.3	96%
*Ec*SlyD*ΔIF	124	11.81 ± 0.36	11.86 ± 0.02	11.4	104%
*Tt*SlyD	154	9.97 ± 0.09	10.37 ± 0.12	10.6	96%
*Tt*SlyDΔIF	111	14.53 ± 0.19	14.89 ± 0.20	11.7	126%
*h*FKBP12	113	13.16 ± 0.08	13.20 ± 0.10	11.7	113%

D indicates diffusion coefficient; aa, number of amino acids. Signal integration for diffusion profiles was performed within the aliphatic (ali; 0.5–2.5 ppm) and amide proton region (aro; 6.5–8.5 ppm) in the ^{1}H spectra. D^{th} represents the theoretical diffusion coefficient for globular proteins according to the number of amino acids [46] and was derived by Eq. (3). *D* represents the average of D^{aro} and D^{ali}.

3.6. NMR titration of Tat peptide (1 17) to EcSlyD* and TtSlyD

Due to the low solubility of the Tat signal peptide (1 27), we used a truncated peptide for the NMR titration experiments containing only the first 17 residues, which comprises the twin arginine motif and most of the conserved hydrophobic region. The fluorescence titration with Tat (1 17) revealed also a 1:1 binding ratio for *Ec*SlyD* and *Tt*SlyD (data not shown). The dissociation constant, K_D, for binding of Tat (1 17) is two orders of magnitude higher compared to Tat (1 27) (Supplementary Fig. SF5 and SF8).

By NMR titration of Tat peptide (1 17) to *Ec*SlyD* and to *Tt*SlyD, we followed the binding site of this peptide to both species of SlyD on a residue by residue basis. As proposed by the fluorescence titration, binding of the Tat peptide (1 17) predominately takes place in both cases at the IF domain (Supplementary Figs. SF4 and SF6, indicated by the highest changes and the number of residues with $\Delta\delta^{all}$ values above a cutoff value of 0.05 ppm and 0.07 ppm, respectively; Supplementary Fig. SF7 provides a color coded structural represen tation of the endpoint of the titration of the Tat peptide (1 17) to *Tt*SlyD).

As a control and for comparison with the fluorescence data, we measured with the Tat peptide (1 27) at very low peptide concentrations (73.5 µM) an F HSQC of 63.5 µM *Tt*SlyDΔIF, which shows no significant chemical shift changes (Supplementary Fig. SF9). This suggests that the additional 10 amino acids of Tat (1 27) versus Tat (1 17) comprise also no FKBP interaction site.

3.7. Backbone dynamics of EcSlyD* and TtSlyD in complex with the Tat peptide (1 17)

To compare the backbone dynamics of free SlyD with the Tat peptide (1 17) bound state, we performed hNOE experiments for the complexes *Ec*SlyD*/Tat (1 17) and *Tt*SlyD/Tat (1 17) (Figs. 1, 6, and 7). The hNOE experiment is an established method to probe qualitatively dynamic changes on the ps to ns time scale at individual sites [54]. As expected, the peptide binding site containing the IF domain shows hNOE values similar or slightly higher for the bound state compared to the free form. This was observed for both the mesophilic and thermophilic species. Surprisingly, *Ec*SlyD* shows significantly reduced hNOE values for G39, L41, and I42 (stick representation in Fig. 1) upon Tat peptide (1 17) binding. The latter two residues belong to the active site for prolyl

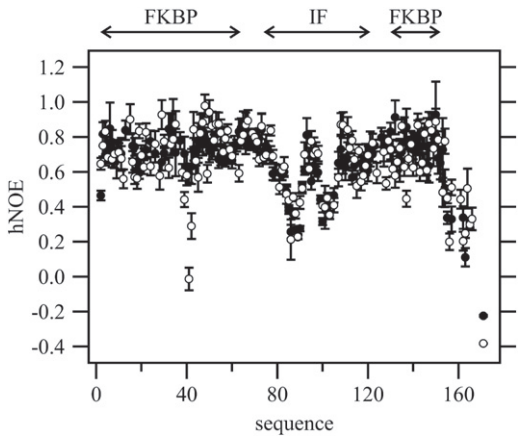

Fig. 6. Heteronuclear steady-state ^{1}H-^{15}N NOE, hNOE, for free *Ec*SlyD* (filled circles) and for Tat peptide (1–17) bound state (open circles) at $T = 298$ K and $B_0 = 14.1$ T. The FKBP domain and the IF domain are indicated at the top.

isomerization of *Ec*SlyD*, which is located in the remote FKBP domain [22]. They become more flexible on the time scale sampled by the hNOE experiment (ps to ns) and belong to the most flexible backbone residues in the complex. In *Tt*SlyD, the corresponding residues are L36 and I37 at the active site. These two residues are shifted in the primary sequence by five positions but are located according to a sequence alignment in the tertiary structure at the same positions [22,24]. Inspection of the hNOE values of *Tt*SlyD in complex with Tat peptide (1 17) reveals increased dynamics for L36 and I37. This agreement of both species is a convincing evidence for a conserved communication mechanism between substrate binding in the IF domain and dynamic changes of the active site in the FKBP domain. Note that the corresponding leucine and isoleucine residues in the FKBP domain show only small changes in chemical shifts for *Ec*SlyD* and slightly more pronounced changes in the case of *Tt*SlyD. Therefore, this communica tion could only be clearly revealed by a comprehensive analysis of protein dynamics by NMR relaxation analysis.

4. Discussion

In this work, we have investigated the global and local dynamics of SlyD, its translational diffusion behavior, and its interactions to a peptide derived from a physiological interaction partner. Both SlyD homologs, *Ec*SlyD* and *Tt*SlyD, consist of two separate domains, which

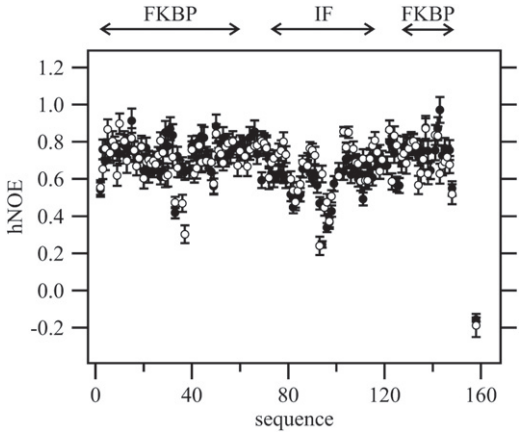

Fig. 7. Heteronuclear steady-state ^{1}H-^{15}N NOE, hNOE, for free *Tt*SlyD (filled circles) and for Tat peptide (1–17) bound state (open circles) at $T = 298$ K and $B_0 = 14.1$ T. The FKBP domain and the IF domain are indicated at the top.

show differences in the local dynamics and changes induced by substrate binding.

We found that the diffusion behavior of SlyD strongly depends on the presence of the IF domain (Table 6). The diffusion coefficients decrease for IF domain deficient SlyD variants and become compa rable to the translational diffusion of *h*FKBP12, representing only the FKBP domain. We conclude that the global molecular shape and the velocity of translational diffusion is directly linked to the presence of the IF domain. Along the same line, the ^{15}N relaxation of the IF domain is not independent from the FKBP domain because its rotational correlation time follows the tumbling of the entire protein.

Our extended data set covering a wide temperature range allows now to compare the proteins from a mesophilic and from a thermophilic organism at different temperatures including the temperatures for optimal growth of both species, which differs by about 30 K. The relaxation rates (higher R_1, lower R_2 rates, and lower hNOE values for the backbone amides in the IF domain compared to the FKBP domain) as well as the dynamic parameters (higher amplitudes of motions and additional fast internal motions of the amides in the IF domain compared to the FKBP domain) showed clearly higher local dynamics of the IF domain compared to the FKBP domain. Here, SlyD from the mesophilic and the thermophilic organism are comparable. This contrasts the observed dynamics of *E. coli*. FkpA, which is also a very efficient prolyl isomerase combined with a second chaperone domain [55]. In this case, both domains show almost identical relaxation rates and hNOE values [56].

The adaptation of thermophilic organisms implies that the biochemical and physiological properties of the proteome remain as functional as in mesophilic organisms. *In vitro*, we can test the physiology of "corresponding states" [57,58] by investigating pairs of mesophilic and thermophilic proteins at a temperature difference corresponding to the difference in the optimal growth temperature. For *E. coli* and *T. thermophilus*, this difference is about 30 °C. At 288 K, the catalytic efficiency of *Tt*SlyD for protein substrates [24] is 2.8 fold reduced compared to $k_{cat}/K_M = 0.82 \times 10^6\ M^{-1}\ s^{-1}$ of *Ec*SlyD* at the same temperature [23,33]. At 303 K, the catalytic efficiency of *Tt*SlyD becomes equal to *Ec*SlyD* (data not shown). Within this temperature range, the molecular tumbling time of *Ec*SlyD* remains about the same (τ_m/η_{buffer} in Table 4) whereas the tumbling time for *Tt*SlyD significantly drops (Table 5) and becomes constant above 313 K. From this observation, we conclude that a τ_m/η_{buffer} value below 13.5 ns goes along with a high catalytic efficiency. Note that a missing IF domain reduces the catalytic efficiency 100 fold for both SlyD homologs.

The binding of a substrate to SlyD was confirmed by fluorescence and by NMR titration experiments. The main binding event takes places in the IF domain, where the highest changes in chemical shift values were observed (up to 0.2 ppm for *Ec*SlyD* and up to 0.15 ppm for *Tt*SlyD). A distinct separation of residues, which sense direct binding during an NMR titration and which sense an induced conformational change far from the binding site, is not possible. Therefore, we performed a second titration with the variants *Ec*SlyD*ΔIF and *Tt*SlyDΔIF, lacking the IF domain. These variants did not bind the Tat signal peptides. Therefore, we suggest that the chemical shift changes for few residues at the FKBP domain are remotely induced conformational changes upon binding of the peptide to the IF domain.

The hNOE relaxation experiments for the substrate bound complexes of *Ec*SlyD* and *Tt*SlyD showed increased dynamics for L41 and I42 for *Ec*SlyD* (center of prolyl peptidyl *cis*/*trans* isomeri zation activity, as shown by mutational studies [23]) and for corresponding L36 and I37 in *Tt*SlyD compared to the free forms. These two residues are clearly pronounced in *Ec*SlyD* from the relaxation data and less obvious from chemical shift changes upon binding. For *Tt*SlyD, both parameters are sensitive. Note that peptide binding affects the internal dynamics probed by hNOE to a much

higher extent compared to changes caused by temperature changes over 15 K for *mesophilic* SlyD and 45 K for *thermophilic* SlyD.

5. Conclusions

The dynamics of the two domain protein SlyD were extensively probed on a ps to ns time scale and in a free as well as substrate bound state. As we detected increased dynamics of active site residues within the FKBP domain upon the remote binding of the substrate to the second domain, we conclude from these results that there has to be a communication between these two domains. This also suggests that the close proximity facilitated by IF domain binding not only increases the catalytic activity of the FKBP domain but also induces changes in the dynamics. The exact mechanism of this interdomain communication needs to be further investigated to compare it with other remote control interactions, for example, for proline switching transmitted by a net of hydrogen bonds [59] or binding of transition state analogs [18].

Acknowledgments

We thank H. Lilie for ultracentrifugation experiments, K. Schröter for usage of the rheometer, and U. Weininger for many helpful discussions. This work was supported by grants from the Deutsche Forschungsgemeinschaft (SFB610) and the Excellence Initiative of the State of Sachsen Anhalt. Significant investments into our NMR facility from the European Regional Development Fund (ERDF) by the European Union are also gratefully acknowledged.

References

[1] H. Frauenfelder, S.G. Sligar, P.G. Wolynes, The energy landscapes and motions of proteins, Science 254 (1991) 1598–1603.
[2] P.W. Fenimore, H. Frauenfelder, B.H. McMahon, F.G. Parak, Slaving: solvent fluctuations dominate protein dynamics and functions, Proc. Natl. Acad. Sci. U. S. A. 99 (2002) 16047–16051.
[3] K.A. Henzler-Wildman, V. Thai, M. Lei, M. Ott, M. Wolf-Watz, T. Fenn, E. Pozharski, M.A. Wilson, G.A. Petsko, M. Karplus, C.G. Hübner, D. Kern, Intrinsic motions along an enzymatic reaction trajectory, Nature 450 (2007) 838–844.
[4] K. Henzler-Wildman, D. Kern, Dynamic personalities of proteins, Nature 450 (2007) 964–972.
[5] A.G. Palmer III, C.D. Kroenke, J.P. Loria, Nuclear magnetic resonance methods for quantifying microsecond-to-millisecond motions in biological macromolecules, Methods Enzymol. 339 (2001) 204–238.
[6] N.A.J. van Nuland, V. Forge, J. Balbach, C.M. Dobson, Real-time NMR studies of protein folding, Acc. Chem. Res. 31 (1998) 773–780.
[7] P. Neudecker, P. Lundström, L.E. Kay, Relaxation dispersion NMR spectroscopy as a tool for detailed studies of protein folding, Biophys. J. 96 (2009) 2045–2054.
[8] Y.W. Bai, J.S. Milne, L. Mayne, S.W. Englander, Protein stability parameters measured by hydrogen exchange, Prot. Struct. Funct. Genet. 20 (1994) 4–14.
[9] M.J. Seewald, K. Pichumani, C. Stowell, B.V. Tibbals, L. Regan, M.J. Stone, The role of backbone conformational heat capacity in protein stability: temperature dependent dynamics of the B1 domain of Streptococcal protein G, Protein Sci. 9 (2000) 1177–1193.
[10] M. Zeeb, M.H. Jacob, T. Schindler, J. Balbach, 15N relaxation study of the cold shock protein CspB at various solvent viscosities, J. Biomol. NMR 27 (2003) 221–234.
[11] D. Canet, P. Barthe, P. Mutzenhardt, C. Roumestand, A comprehensive analysis of multifield 15N relaxation parameters in proteins: determination of 15N chemical shift anisotropies, J. Am. Chem. Soc. 123 (2001) 4567–4576.
[12] K.B. Wong, A.R. Fersht, S.M. Freund, NMR 15N relaxation and structural studies reveal slow conformational exchange in barstar C40/82A, J. Mol. Biol. 268 (1997) 494–511.
[13] K.A. Henzler-Wildman, M. Lei, V. Thai, S.J. Kerns, M. Karplus, D. Kern, A hierarchy of timescales in protein dynamics is linked to enzyme catalysis, Nature 450 (2007) 913–916.
[14] N.A. Temiz, E. Meirovitch, I. Bahar, *Escherichia coli* adenylate kinase dynamics: comparison of elastic network model modes with mode-coupling 15N-NMR relaxation data, Prot. Struct. Funct. Bioinformat. 57 (2004) 468–480.
[15] P. Bernadó, M.X. Fernandes, D.M. Jacobs, K. Fiebig, J. García de la Torre, M. Pons, Interpretation of NMR relaxation properties of Pin1, a two-domain protein, based on Brownian dynamic simulations, J. Biomol. NMR 29 (2004) 21–35.
[16] G. Hofmann, K. Schweimer, A. Kiessling, E. Hofinger, F. Bauer, S. Hoffmann, P. Rösch, I.D. Campbell, J.M. Werner, H. Sticht, Binding, domain orientation, and dynamics of the Lck SH3–SH2 domain pair and comparison with other Src-family kinases, Biochemistry 44 (2005) 13043–13050.
[17] I.-J.L. Byeon, K.K. Dao, J. Jung, J. Keen, I. Leiros, S.O. Doskeland, A. Martinez, A.M. Gronenborn, Allosteric communication between cAMP binding sites in the RI subunit of protein kinase A revealed by NMR, J. Biol. Chem. 285 (2010) 14062–14070.
[18] J.P. Marston, M.J. Cliff, M.A.C. Reed, G.M. Blackburn, A.M. Hounslow, C.J. Craven, J.P. Waltho, Structural tightening and interdomain communication in the catalytic cycle of phosphoglycerate kinase, J. Mol. Biol. 396 (2010) 345–360.
[19] J. Fanghänel, G. Fischer, Insights into the catalytic mechanism of peptidyl prolyl cis/trans isomerases, Front. Biosci. 9 (2004) 3453–3478.
[20] W.D. Roof, S.M. Horne, K.D. Young, R. Young, SlyD, a host gene required for phi X174 lysis, is related to the FK506-binding protein family of peptidyl-prolyl cis–trans-isomerases, J. Biol. Chem. 269 (1994) 2902–2910.
[21] S. Hottenrott, T. Schumann, A. Plückthun, G. Fischer, J.U. Rahfeld, The *Escherichia coli* SlyD is a metal ion-regulated peptidyl-prolyl cis/trans-isomerase, J. Biol. Chem. 272 (1997) 15697–15701.
[22] U. Weininger, C. Haupt, K. Schweimer, W. Graubner, M. Kovermann, T. Brüser, C. Scholz, P. Schaarschmidt, G. Zoldak, F.X. Schmid, J. Balbach, NMR solution structure of SlyD from *Escherichia coli*: spatial separation of prolyl isomerase and chaperone function, J. Mol. Biol. 387 (2009) 295–305.
[23] C. Scholz, B. Eckert, F. Hagn, P. Schaarschmidt, J. Balbach, F.X. Schmid, SlyD proteins from different species exhibit high prolyl isomerase and chaperone activities, Biochemistry 45 (2006) 20–33.
[24] C. Löw, P. Neumann, H. Tidow, U. Weininger, C. Haupt, B. Friedrich-Epler, C. Scholz, M.T. Stubbs, J. Balbach, Crystal structure determination and functional characterization of the metallochaperone SlyD from *Thermus thermophilus*, J. Mol. Biol. 398 (2010) 375–390.
[25] L. Martino, Y. He, K.L.D. Hands-Taylor, E.R. Valentine, G. Kelly, C. Giancola, M.R. Conte, The interaction of the *Escherichia coli* protein SlyD with nickel ions illuminates the mechanism of regulation of its peptidyl-prolyl isomerase activity, FEBS J. 276 (2009) 4529–4544.
[26] G. Zoldak, L. Carstensen, C. Scholz, F.X. Schmid, Consequences of domain insertion on the stability and folding mechanism of a protein, J. Mol. Biol. 386 (2009) 1138–1152.
[27] R.P. Jakob, G. Zoldak, T. Aumüller, F.X. Schmid, Chaperone domains convert prolyl isomerases into generic catalysts of protein folding, Proc. Natl. Acad. Sci. U. S. A. 106 (2009) 20282–20287.
[28] W. Graubner, A. Schierhorn, T. Brüser, DnaK plays a pivotal role in Tat targeting of CueO and functions beside SlyD as a general Tat signal binding chaperone, J. Biol. Chem. 282 (2007) 7116–7124.
[29] G.M. Clore, A. Szabo, A. Bax, L.E. Kay, P.C. Driscoll, A.M. Gronenborn, Deviations from the simple two-parameter model-free approach to the interpretation of nitrogen-15 nuclear magnetic relaxation of proteins, J. Am. Chem. Soc. 112 (1990) 4989–4991.
[30] G. Lipari, A. Szabo, Model-free approach to the interpretation of nuclear magnetic resonance relaxation in macromolecules. 2. Analysis of experimental results, J. Am. Chem. Soc. 104 (1982) 4559–4570.
[31] G. Lipari, A. Szabo, Model-free approach to the interpretation of nuclear magnetic resonance relaxation in macromolecules. 1. Theory and range of validity, J. Am. Chem. Soc. 104 (1982) 4546–4559.
[32] J.A. Jones, D.K. Wilkins, L.J. Smith, C.M. Dobson, Characterisation of protein unfolding by NMR diffusion measurements, J. Biomol. NMR 10 (1997) 199–203.
[33] T.A. Knappe, B. Eckert, P. Schaarschmidt, C. Scholz, F.X. Schmid, Insertion of a chaperone domain converts FKBP12 into a powerful catalyst of protein folding, J. Mol. Biol. 368 (2007) 1458–1468.
[34] K. Dayie, G. Wagner, Relaxation-rate measurements for 15N-1H groups with pulsed-field gradients and preservation of coherence pathways, J. Magn. Reson. A 111 (1994) 121–126.
[35] L.E. Kay, D.A. Torchia, A. Bax, Backbone dynamics of proteins as studied by 15N inverse detected heteronuclear NMR spectroscopy: application to staphylococcal nuclease, Biochemistry 28 (1989) 8972–8979.
[36] F. Delaglio, S. Grzesiek, G.W. Vuister, G. Zhu, J. Pfeifer, A. Bax, NMRPipe: a multidimensional spectral processing system based on UNIX pipes, J. Biomol. NMR 6 (1995) 277–293.
[37] B.A. Johnson, R.A. Blevins, NMRView: a computer program for visualization and analysis of NMR data, J. Biomol. NMR 4 (1994) 603–614.
[38] A.G. Palmer III, M. Rance, P.E. Wright, Intramolecular motions of a zinc finger DNA-binding domain from Xfin characterized by proton detected natural abundance C-13 heteronuclear NMR spectroscopy, J. Am. Chem. Soc. 113 (1991) 4371–4380.
[39] A.M. Mandel, M. Akke, A.G. Palmer III, Backbone dynamics of *Escherichia coli* ribonuclease HI: correlations with structure and function in an active enzyme, J. Mol. Biol. 246 (1995) 144–163.
[40] A. Abragam, Principles of Nuclear Magnetism, Clarendon Press, Oxford, 1961.
[41] Y. Hiyama, C.H. Niu, J.V. Silverton, A. Bavoso, D.A. Torchia, Determination of ^{15}N chemical shift tensor via ^{15}N-^{2}H dipolar coupling in Boc-glycylglycyl[^{15}N]glycine benzyl ester, J. Am. Chem. Soc. 110 (1988) 2378–2383.
[42] P. Dosset, J.-C. Hus, M. Blackledge, D. Marion, Efficient analysis of macromolecular rotational diffusion from heteronuclear relaxation data, J. Biomol. NMR 16 (2000) 23–28.
[43] Y.C. Li, G.T. Montelione, Human type-alpha transforming growth factor undergoes slow conformational exchange between multiple backbone conformations as

characterized by nitrogen-15 relaxation measurements, Biochemistry 34 (1995) 2408–2423.
[44] S. Berger, 200 NMR Experiments, WILEY-VCH, Weinheim, 2002.
[45] J. Balbach, Compaction during protein folding reactions studied by real-time NMR diffusion experiments, J. Am. Chem. Soc. 122 (2000) 5887–5888.
[46] D.K. Wilkins, S.B. Grimshaw, V. Receveur, C.M. Dobson, J.A. Jones, L.J. Smith, Hydrodynamic radii of native and denatured proteins measured by pulse field gradient NMR techniques, Biochemistry 38 (1999) 16424–16431.
[47] A. Einstein, Über die von der molekularkinetischen Theorie der Wärme geforderte Bewegung von in ruhenden Flüssigkeiten suspendierten Teilchen, Ann. Phys. 17 (1905) 549–560.
[48] S. Mori, C. Abeygunawardana, M.O. Johnson, P.C. van Zijl, Improved sensitivity of HSQC spectra of exchanging protons at short interscan delays using a new fast HSQC (FHSQC) detection scheme that avoids water saturation, J. Magn. Reson. B 108 (1995) 94–98.
[49] S. Grzesiek, S.J. Stahl, P.T. Wingfield, A. Bax, The CD4 determinant for down-regulation by HIV-1 Nef directly binds to Nef. Mapping of the Nef binding surface by NMR, Biochemistry 35 (1996) 10256–10261.
[50] C. Scholz, P. Schaarschmidt, A.M. Engel, H. Andres, U. Schmitt, E. Faatz, J. Balbach, F.X. Schmid, Functional solubilization of aggregation-prone HIV envelope proteins by covalent fusion with chaperone modules, J. Mol. Biol. 345 (2005) 1229–1241.
[51] N. Bloembergen, E.M. Purcell, R.V. Pound, Relaxation effects in nuclear magnetic resonance absorption, Phys. Rev. 73 (1948) 679.
[52] M. Weiwad, A. Werner, P. Rucknagel, A. Schierhorn, G. Kullertz, G. Fischer, Catalysis of proline-directed protein phosphorylation by peptidyl-prolyl cis/trans isomerases, J. Mol. Biol. 339 (2004) 635–646.
[53] A. Galat, S.M. Metcalfe, Peptidylproline cis/trans isomerases, Progr. Biophys. Mol. Biol. 63 (1995) 67–118.
[54] S. Ramboarina, C. Redfield, Probing the effect of temperature on the backbone dynamics of the human a-lactalbumin molten globule, J. Am. Chem. Soc. 130 (2008) 15318–15326.
[55] K. Ramm, A. Plückthun, High enzymatic activity and chaperone function are mechanistically related features of the dimeric *E. coli* peptidyl-prolyl-isomerase FkpA, J. Mol. Biol. 310 (2001) 485–498.
[56] K. Hu, V. Galius, K. Pervushin, Structural plasticity of peptidyl-prolyl isomerase sFkpA is a key to its chaperone function as revealed by solution NMR, Biochemistry 45 (2006) 11983–11991.
[57] G.N. Somero, Proteins and temperature, Ann. Rev. Physiol. 57 (2003) 43–68.
[58] R. Jaenicke, Stability and stabilization of globular proteins in solution, J. Biotechnol. 79 (2000) 193–203.
[59] U. Weininger, R.P. Jakob, B. Eckert, K. Schweimer, F.X. Schmid, J. Balbach, A remote prolyl isomerization controls domain assembly via a hydrogen bonding network, Proc. Natl. Acad. Sci. U. S. A. 106 (2009) 12335–12340.